

Multi-Depth Boundary-Aware Left Atrial Scar Segmentation Network

Mengjun Wu*, Wangbin Ding*, Mingjin Yang (✉), and Liqin Huang

College of Physics and Information Engineering, Fuzhou University, Fuzhou, China
yangmj5@fzu.edu.cn

Abstract. Automatic segmentation of left atrial (LA) scars from late gadolinium enhanced CMR images is a crucial step for atrial fibrillation (AF) recurrence analysis. However, delineating LA scars is tedious and error-prone due to the variation of scar shapes. In this work, we propose a boundary-aware LA scar segmentation network, which is composed of two branches to segment LA and LA scars, respectively. We explore the inherent spatial relationship between LA and LA scars. By introducing a Sobel fusion module between the two segmentation branches, the spatial information of LA boundaries can be propagated from the LA branch to the scar branch. Thus, LA scar segmentation can be performed condition on the LA boundaries regions. In our experiments, 40 labeled images were used to train the proposed network, and the remaining 20 labeled images were used for evaluation. The network achieved an average Dice score of 0.608 for LA scar segmentation.

Keywords: Left Atrial Scar · Multi-Depth Segmentation · Boundary-Aware.

1 Introduction

Atrial fibrillation (AF) is the most common arrhythmia, occurring at any age, from children to the elderly [3]. Clinically, catheter ablation (CA) [8] is a widely used invasive procedure for AF treatment, but with a 45% recurrence rate [1]. Recent studies demonstrated the relationship between the recurrence of AF and left atrial (LA) scars after CA [15,5]. Late gadolinium enhanced (LGE) cardiac MR has emerged as one of the promising techniques for imaging LA scars [14]. Delineating scarring regions from LGE images could analyze the formation of LA scars, and benefit the monitoring and management of AF patients.

Conventional scar segmentation methods are mainly based on thresholding, region-growing and graph-cut algorithms [7]. Deep-learning (DL) based methods have recently been widely studied for LA scar segmentation tasks. Most DL-based methods explore employing LA or LA walls to improve the scar segmentation. For instance, Chen *et al.*[2] presented a multi-task segmentation methods, where LA and scars were jointly predicted with an attention model; Li *et al.*[9,11]

* The two authors have equal contributions to the paper.

formulated the spatial relationship between LA walls and scars as loss function, which could force the network to focus on objective regions during inference.

Generally, the size of LA scars is varied largely. In the training dataset of LAscarQS 2022 [11,12,10], each LGE image contains average 41.17 scars, and the size of scars are ranged from 0.98 mm³ to 7545.89 mm³. Table 1 presents the statistical information of the scars in LAscarQS 2022. One can observe, 76.1% of scars sizes are within 50 mm³, and they occupy 16.17% of total scars volume; whereas only 2.8% of scars sizes are larger than 500 mm³, but they cover 48% of total scars volume in the whole dataset. For the tiny objects, a shallower network could outperform the deep U-Net; For the large objects, a deeper network could outperform the shallower network [16]. The optimal depth of a segmentation network can vary due to the variety of sizes, which poses an additional challenge in performing scar segmentation.

Table 1. statistical information of scarring regions in the training dataset of LAscarQS2022

Range (mm ³)	0-50	50-100	100-150	150-200	200-250	250-300	300-350	350-400	400-450	450-500	>500
Number of Scar	1881	262	121	39	24	17	20	14	14	7	71
Percentage (%)	76.15	10.61	4.89	1.58	0.97	0.69	0.809	0.566	0.566	0.28	2.87
Total Number	2470										
Scar Volume	33014	18624	14981	6778	5237	4632	6510	5273	5898	3321	99918
Percentage (%)	16.17	9.12	7.34	3.32	2.56	2.27	3.19	2.58	2.89	1.626	48.93
Total Scar Volume	204191										

As shown in Figure 1, we propose a multi-depth boundary-aware network, namely MDBAnet, to segment different sizes of LA scars. The main contribution of this work includes: (1) We present a multi-depth segmentation network to segment multiple sizes of scars. (2) We propose a plug-and-play Sobel [13] fusion module, which aims to extract LA boundary information to improve scar segmentation.

2 Method

2.1 Network Architecture

MDBAnet comprises two branches, which segment LA and LA scars, respectively. Scars are distributed on the LA wall, and the size of scars varies largely, as seen from our statistical information (Table 1). In order to achieve scar segmentation of different sizes, the scar branch is stacked with multiple U-Nets that share the same encoder but with different decoder depths. We expect that the shallow networks will focus on segmenting small-size scars, while the deep networks will focus on segmenting large-size scars. Finally, we fuse segmentation results of each U-Net as follows:

$$\hat{Y}_{Scar} = \frac{1}{N} \sum_{n=1}^N \hat{Y}_n \quad (1)$$

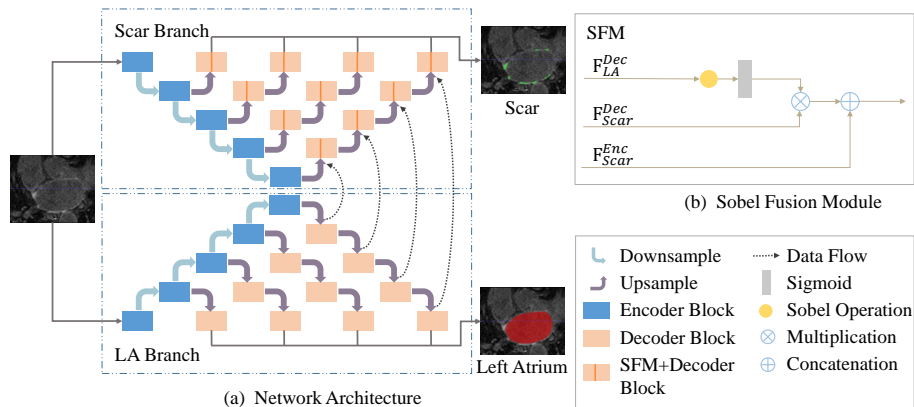


Fig. 1. The architecture of multi-depth boundary-aware network (MDBAnet). It consists of two segmentation branches, i.e., the scar branch and the left atrial (LA) branch. In both branches, we introduce multiple U-Nets with different depths to perform scar and LA segmentation. Furthermore, we propose a Sobel fusion module to extract and propagate LA boundaries information from the LA branch to the scar branch. For conciseness, we only reserve the data flow between the deepest LA decoder path and scar decoder, and all skip connections are omitted.

where N is the number of U-Nets with different depths, and \hat{Y}_n is the output of the corresponding U-Net.

Furthermore, we aim to improve the performance of scar segmentation by jointly performing LA segmentation. Thus, as shown in Figure 1, we introduce the LA branch for LA segmentation. The network architecture of the LA branch is symmetric to the scar branch, which is stacked with multiple U-Nets. It outputs LA regions for LGE images.

2.2 Sobel Fusion Module

We explore the inherent spatial relationship between LA and LA scars. Generally, LA scars are distributed around LA boundaries. We introduce a Sobel [6] operator to extract the boundary information of feature maps. Then a Sobel fusion module (SFM) is proposed to take full advantage of the spatial relationship between boundary information and LA scars. The input of SFM includes the feature maps of LA decoder, the previous layer of scar decoder and scar encoder. The output of SFM can be calculated as follows:

$$F^{out} = (F_{Scar}^{Dec} \otimes S(F_{LA}^{Dec})) \oplus F_{Scar}^{Enc}, \quad (2)$$

where \otimes and \oplus represent element-wise multiplication and concatenation, respectively, S represents 3D Sobel operation, F^{Enc} and F^{Dec} are the feature map from the encoder path and decoder path, respectively. Here, Sobel operation is

implemented by a fixed kernel convolution layer, which consists of three 3D Sobel kernels. Following Xu *et al.*[13], each 3D Sobel Kernel can be described as a $3 \times 3 \times 3$ matrix, as shown in Figure 2. They can be used to extract the boundary information from the axial, sagittal and coronal views of image.

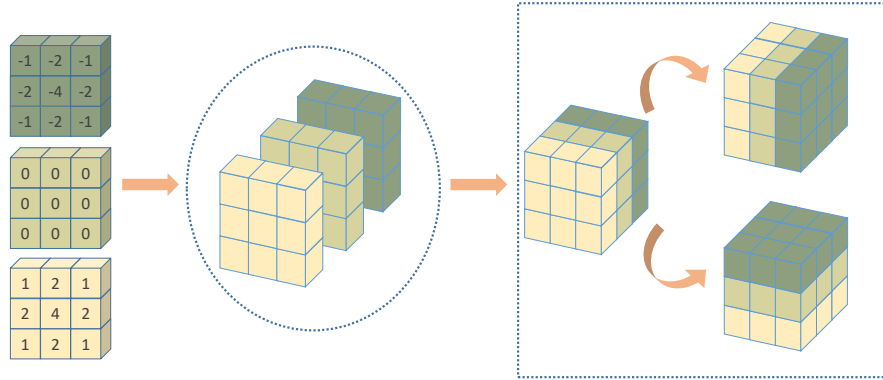


Fig. 2. Our 3D Sobel kernel

Based on the SFM, the feature map from the decoder path of the LA branch could be passed to the 3D Sobel Kernel to get the boundary information of LA. Then we re-calibrate the feature map of the scar branch with the boundary information, which provides spatial attention and forces the network to focus on the LA boundaries region.

2.3 Loss Function

We employ Dice loss and cross-entropy loss to jointly optimize the segmentation results of the network. The total loss of our network is:

$$\begin{aligned} \mathcal{L} = & -DCS(\hat{Y}_{Scar}, Y_{Scar}) + CE(\hat{Y}_{Scar}, Y_{Scar}) \\ & -DCS(\hat{Y}_{LA}, Y_{LA}) + CE(\hat{Y}_{LA}, Y_{LA}), \end{aligned} \quad (3)$$

where $\hat{Y}_{\{Scar, LA\}}$ and $Y_{\{Scar, LA\}}$ are the predicted and gold standard labels, respectively; $DCS(a, b)$ calculate the Dice score (DS) between a and b; and $CE(a, b)$ calculate the cross-entropy loss.

3 Experiment

3.1 Dataset

We trained and evaluated our method on the Left Atrial and Scar Quantification & Segmentation Challenge 2022 (LAScarQS 2022) dataset, which aimed

to segment LA and LA scars from LGE CMR images. The challenge dataset provides a total of 60 labeled and 10 unlabeled LGE CMR images, and gold standard labels include: LA and LA scars. In our experiment, we split the labeled images into a training set of 40 cases, and the remaining 20 cases for evaluation. Finally, the performance of the network was evaluated on 10 unlabeled images.

3.2 Implementations

Our network was implemented in PyTorch, using two NVIDIA GeForce RTX 3080 GPUs. We used SGD optimizer to adjust the network parameters (batch size=2, weight decay=0.00003, momentum=0.99). The initial learning rate was set 0.01 and decayed exponentially. During training, enhancement techniques, i.e., random rotation, random scaling, random elastic deformation, gamma-corrected enhancement and mirroring, were applied on the fly.

3.3 Result

We compared our method to three different segmentation methods:

- nnU-Net [4]: One of the state-of-the-art segmentation networks. We trained it with 3D LGE images as well as corresponding scar labels.
- MDnet: A multi-depth segmentation network based on U-Net, which is the scar branch of MDBAnet.
- MDBAnet_{mul}: A variation of MDBAnet. We implement a multiplication fusion module to propagate information from the LA branch to the scar branch.
- MDBAnet: The proposed network. It consists two branches with multi-depth network to segment LA and scars. We implement a Sobel fusion module to propagate information from the LA branch to the scar branch.

To evaluate methods, DS and Hausdorff distance (HD) were calculated between the prediction results and the gold standard label.

Table 2. The performance of different methods. DS: Dice score; HD: Hausdorff distance. Note that MDBAnet and MDBAnet_{mul} jointly produce scar and LA segmentation, we thus list the LA segmentation results of this two methods.

Methods	LA		Scar	
	DS	HD (mm)	DS	HD (mm)
nnU-Net	-	-	0.488(0.090)	39.62(12.81)
MDnet	-	-	0.504(0.085)	40.66(12.88)
MDBAnet _{mul}	0.926(0.020)	17.83(11.33)	0.504(0.087)	33.21(10.43)
MDBAnet	0.923(0.027)	19.18(11.10)	0.512(0.083)	31.67(10.86)

Table 2 shows the segmentation performance of different methods. Methods using a multi-depth strategy (i.e., MDBAnet, MDBAnet_{mul} and MDnet) had

obtained better segmentation performance compared to single-depth network, i.e., nnU-Net. Particularly, MDnet improved Dice and HD by 0.01 and 1 for scar segmentation, respectively. It proves the effectiveness of using multi-depth strategy. Meanwhile, scar segmentation could be further improved by jointly performing LA segmentation. One can see that both MDBAnet_{mul} and MDBAnet improve the scar segmentation results by utilizing information from the LA branch. For example, MDBAnet achieved an improvement DS by 0.8% ($p=0.125$), and significantly reduced HD from 40.66 to 31.67 ($p<0.05$) against MDnet. Besides, MDBAnet_{mul} propagated the entire feature maps of the LA branch, while the MDBAnet extracted the boundary information via SFM. MDBAnet could obtain better DS and HD for scar segmentation. This implied the benefit of SFM.

In Figure 3, we showed four typical cases for visualization. nnU-Net may failed to perform segmentation for tiny scars (yellow Boxes), which is consist to the quantity result of Table 2. Moreover, MDBAnet achieved better results for some difficult cases, such as ambiguity scars (yellow Arrows). This was probably due to the usage of SFM, which could force the scar branch to focus on boundary regions.

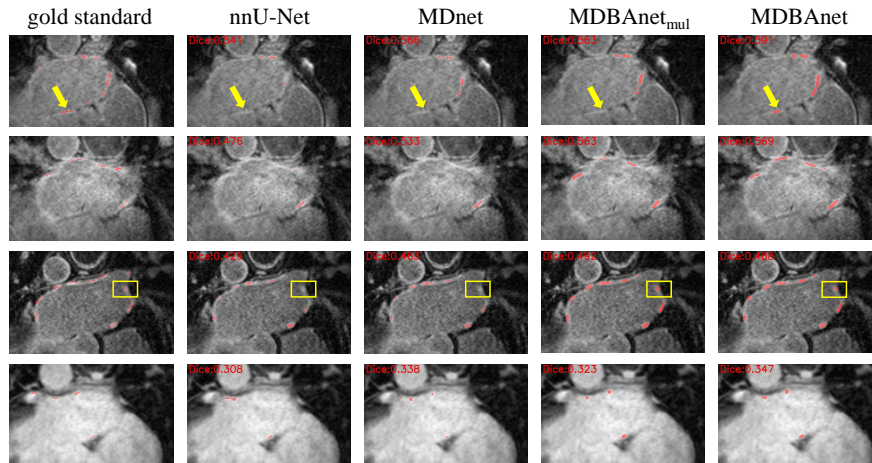


Fig. 3. Visualization of different scar segmentation methods. Yellow Arrows mark the advantage of MDBAnet, while yellow Boxes denote the tiny scars.

4 Conclusion

In this work, we have proposed a multi-depth boundary-aware LA scar segmentation network. It consists of two segmentation branches based on multi-depth strategy. Meanwhile, we implemented a SFM to propagate information

from LA branch to scar branch. The experimental results showed that multi-depth network has a positive effect on scar segmentation, and SFM was capable of further improving scar segmentation performance. The network achieved a DS of 0.608 on validation data of LAScarQS 2022.

References

1. Balk, E.M., Garlitski, A.C., ALSHEIKH-ALI, A.A., Terasawa, T., Chung, M., Ip, S.: Predictors of atrial fibrillation recurrence after radiofrequency catheter ablation: a systematic review. *Journal of cardiovascular electrophysiology* **21**(11), 1208–1216 (2010)
2. Chen, J., Yang, G., Gao, Z., Ni, H., Angelini, E., Mohiaddin, R., Wong, T., Zhang, Y., Du, X., Zhang, H., et al.: Multiview two-task recursive attention model for left atrium and atrial scars segmentation. In: *International Conference on Medical Image Computing and Computer-Assisted Intervention*. pp. 455–463. Springer (2018)
3. Heeringa, J., van der Kuip, D.A., Hofman, A., Kors, J.A., van Herpen, G., Stricker, B.H.C., Stijnen, T., Lip, G.Y., Wittteman, J.C.: Prevalence, incidence and lifetime risk of atrial fibrillation: the rotterdam study. *European heart journal* **27**(8), 949–953 (2006)
4. Isensee, F., Petersen, J., Klein, A., Zimmerer, D., Jaeger, P.F., Kohl, S., Wasserthal, J., Koehler, G., Norajitra, T., Wirkert, S., et al.: nnu-net: Self-adapting framework for u-net-based medical image segmentation. *arXiv preprint arXiv:1809.10486* (2018)
5. Jefairi, N.A., Camaioni, C., Sridi, S., Cheniti, G., Takigawa, M., Nivet, H., Denis, A., Derval, N., Merle, M., Laurent, F., et al.: Relationship between atrial scar on cardiac magnetic resonance and pulmonary vein reconnection after catheter ablation for paroxysmal atrial fibrillation. *Journal of Cardiovascular Electrophysiology* **30**(5), 727–740 (2019)
6. Kanopoulos, N., Vasanthavada, N., Baker, R.L.: Design of an image edge detection filter using the sobel operator. *IEEE Journal of solid-state circuits* **23**(2), 358–367 (1988)
7. Karim, R., Housden, R.J., Balasubramaniam, M., Chen, Z., Perry, D., Uddin, A., Al-Beyatti, Y., Palkhi, E., Acheampong, P., Obom, S., et al.: Evaluation of current algorithms for segmentation of scar tissue from late gadolinium enhancement cardiovascular magnetic resonance of the left atrium: an open-access grand challenge. *Journal of Cardiovascular Magnetic Resonance* **15**(1), 1–17 (2013)
8. Kirchhof, P., Calkins, H.: Catheter ablation in patients with persistent atrial fibrillation. *European heart journal* **38**(1), 20–26 (2017)
9. Li, L., Weng, X., Schnabel, J.A., Zhuang, X.: Joint left atrial segmentation and scar quantification based on a dnn with spatial encoding and shape attention. In: *International Conference on Medical Image Computing and Computer-Assisted Intervention*. pp. 118–127. Springer (2020)
10. Li, L., Zimmer, V.A., Schnabel, J.A., Zhuang, X.: Atrialgeneral: Domain generalization for left atrial segmentation of multi-center lge mris. In: *International Conference on Medical Image Computing and Computer-Assisted Intervention*. pp. 557–566. Springer (2021)
11. Li, L., Zimmer, V.A., Schnabel, J.A., Zhuang, X.: Atrialjsqnet: A new framework for joint segmentation and quantification of left atrium and scars incorporating spatial and shape information. *Medical Image Analysis* **76**, 102303 (2022)

12. Li, L., Zimmer, V.A., Schnabel, J.A., Zhuang, X.: Medical image analysis on left atrial lge mri for atrial fibrillation studies: A review. *Medical Image Analysis* p. 102360 (2022)
13. Xu, Z., Wu, Z., Feng, J.: Cfun: Combining faster r-cnn and u-net network for efficient whole heart segmentation. *arXiv preprint arXiv:1812.04914* (2018)
14. Yang, G., Chen, J., Gao, Z., Li, S., Ni, H., Angelini, E., Wong, T., Mohiaddin, R., Nyktari, E., Wage, R., et al.: Simultaneous left atrium anatomy and scar segmentations via deep learning in multiview information with attention. *Future Generation Computer Systems* **107**, 215–228 (2020)
15. Zghaib, T., Nazarian, S.: New insights into the use of cardiac magnetic resonance imaging to guide decision making in atrial fibrillation management. *Canadian Journal of Cardiology* **34**(11), 1461–1470 (2018)
16. Zhou, Z., Siddiquee, M.M.R., Tajbakhsh, N., Liang, J.: Unet++: Redesigning skip connections to exploit multiscale features in image segmentation. *IEEE transactions on medical imaging* **39**(6), 1856–1867 (2019)